

# The Tails of the crossing probability

Oleg A.Vasilyev<sup>1,2\*</sup>

<sup>1</sup> *Laboratoire de Physique Théorique de la Matière Condensée,  
Université Paris-VI, 75252 Paris Cedex 05, France*

<sup>2</sup> *L.D.Landau Institute for Theoretical Physics RAS,  
142432, Chernogolovka, Moscow reg., Russia*

(Dated: November 21, 2018)

The scaling of the tails of the probability of a system to percolate only in the horizontal direction  $\pi_{hs}$  was investigated numerically for correlated site-bond percolation model for  $q = 1, 2, 3, 4$ . We have to demonstrate that the tails of the crossing probability far from the critical point  $p_c$  have shape  $\pi_{hs}(p) \simeq D \exp(cL [p - p_c]^\nu)$  where  $\nu$  is the correlation length index,  $p = 1 - \exp(-\beta)$  is the probability of a bond to be closed. At criticality we observe crossover to another scaling  $\pi_{hs}(p) \simeq A \exp(-b \{L[p - p_c]^\nu\}^z)$ . Here  $z$  is a scaling index describing the central part of the crossing probability.

## I. INTRODUCTION

The  $q$ -state Potts model can be represented as the correlated site-bond percolation in terms of Fortuin-Kasteleyn clusters [1]. At the critical point of the second order phase transition, the infinite cluster is formed. This cluster crosses the system connecting the opposite sides of the square lattice. In the last decade the study of the shape of the crossing probability was performed by conformal methods [2, 3, 4, 5, 6, 7] as well as numerically [8, 9, 10, 11, 12, 13, 14, 15, 16, 17].

According to Refs. [18, 19] the distribution function of the percolation thresholds is Gaussian function. Following the number of works [10, 16, 17, 20, 21] the tails of the distribution function are not Gaussian ones. The authors of the recent work Ref. [22] are still uncertain to distinguish a stretched exponential behavior from a Gaussian.

---

\*Electronic address: vasilyev@itp.ac.ru

The aim of this paper is to investigate the shape of the probability of a system to percolate only in horizontal direction  $\pi_{hs}$ . We perform numerical simulation of correlated site-bond percolation model for  $q = 1, 2, 3, 4$  (the percolation model  $q = 1$ , the Ising model  $q = 2$  and the Potts model  $q = 3, 4$ ) for lattice sizes  $L = 32, 48, 64, 80, 128$ . The scaling formulas for a body of the crossing probability at criticality and for tails of the crossing probability were obtained. The final result for the representative case  $q = 2, L = 128$  is immediately presented in Fig. 1a). Details of fitting procedure are described in Section V. In this figure

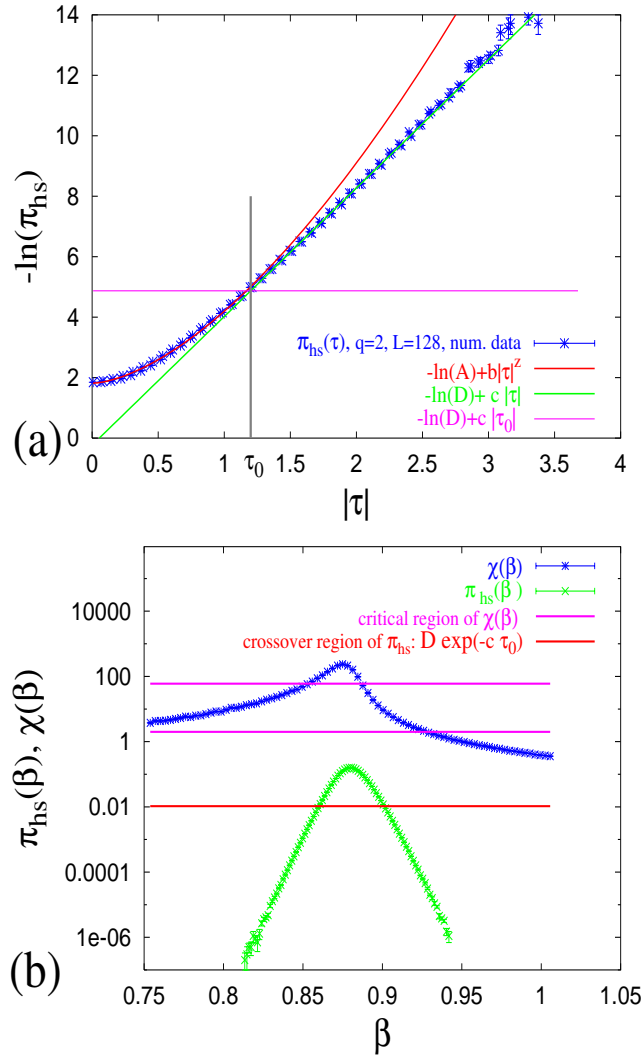


FIG. 1: a) The absolute value of the logarithm of the crossing probability  $-\ln(\pi_{hs})$  for the Ising model as a function of the absolute value of the scaling variable  $\tau = L(p - p_c)^\nu$  on the lattice  $L = 128$ ; b) The magnetic susceptibility  $\chi(\beta)$  and the crossing probability  $\pi_h(\beta)$  as a functions of the inverse temperature  $\beta$  for the Ising model,  $L = 128$ .

we plot (by crosses) the numerical data for the absolute value of the logarithm of crossing probability  $\pi_{hs}$  for the Ising model ( $q = 2$ ) on the lattice  $L = 128$  as a function of the absolute value of the scaling variable  $\tau = L(p - p_c)^\nu$ . Here  $p = 1 - \exp(-\beta)$  is a probability of a bond to be closed,  $\beta$  is the inverse temperature,  $\nu$  is the correlation length scaling index. The critical point in the  $p$  scale for the  $q$ -state Potts model is  $p_c = \sqrt{q}/(1 + \sqrt{q})$  see Ref. [23] and we get  $p_c(q = 2) \simeq 0.58578\dots$

We can see from Fig. 1a) that the function  $\pi_{hs}(\tau)$  consists of two parts: the body  $|\tau| < \tau_0$  and the tails  $|\tau| > \tau_0$ . The negative logarithm of the body of the crossing probability as a function of  $\tau$  is well described by function  $-\ln(A) + b|\tau|^z$  (solid line on the Fig. 1a)). Here  $z$  is some scaling index. The value of the crossing probability at the critical point  $\pi_{hs}(p_c) = A$  may be computed (at least for percolation) by conformal field methods [4]. The negative logarithm of the tails of the crossing probability have shape  $-\ln(D) + c\tau$  (dashed line in the Fig. 1a)). This line is tangent to the body at the point  $\tau_0$ . This point is marked by the horizontal line. Let us note that in Fig. 1a) we plot two branches of the crossing probability (for  $\tau > 0$  and  $\tau < 0$ ). The coincidence of this two branches indicate the remarkable symmetry of the crossing probability with respect to the variable  $\tau$ .

In Fig. 1b) we plot the crossing probability by crosses (bottom) and the magnetic susceptibility by triangles (top) as a functions of the inverse temperature  $\beta$  with logarithm scale for the ordinate axis. In Fig. 1b) we indicate the position of crossover region of  $\pi_{hs}$  by horizontal solid line on a level  $D \exp(-c\tau_0)$ . For the magnetic susceptibility we mark the region with critical behavior

$$\chi(\beta) \sim ((\beta - \beta_c)/\beta_c)^{-\gamma} \quad (1)$$

by horizontal dashed lines. We see from Fig. 1b) that tails of the crossing probability directly correspond to the critical region of the magnetic susceptibility. In this critical region the correlation length  $\xi$  is smaller than the sample size  $\xi < L$ . As the temperature approaches to the critical point, the correlation length reaches the sample size. At that point the magnetic susceptibility on the finite lattice deviates from the critical behavior Eq. (1) and becomes smooth – see the region over the top dashed horizontal line in the Fig. 1b). At the same point the crossing probability crosses over from tails to body – the region over the solid horizontal line in Fig. 1b) (and the region *under* the horizontal line in Fig. 1a)). At the critical point  $\beta_c = -\ln(1 - p_c) \simeq 0.881373\dots$  both the magnetic susceptibility and the crossing probability reach a maximum.

The detailed description of the fitting procedure as well as numerical data for  $q = 1, 2, 3, 4$  are presented below. The main numerical result of this paper is the proving of the formula  $D \exp(b[p-p_c]L^\nu)$  for the tails of the crossing probability. Therefore, we pay special attention to fitting procedures.

The paper is organized as follows: In the second section, we describe details of the numerical simulation. In the third section, the method for determining the pseudocritical point  $p_c(L, q)$  on the finite lattice is described. We use  $p_c(L, q)$  to perform the approximation of the tails. In section IV we approximate the double logarithm of the crossing probability  $\ln(-\ln(\pi_{hs}(p; L, q)))$  tails as a function of the logarithm of deviation from the critical point  $\ln(p - p_c(L, q))$  by the linear function  $\tilde{c}(L, q) + x(L, q) \ln(p - p_c(L, q))$ . We get  $x(L, q) \simeq \nu(q)$  for this approximation procedure. In section V we describe new fitting procedure using the scaling variable  $\tau = L(p - p_c)^\nu$ . Results of approximation are discussed in Section VI.

## II. DETAILS OF NUMERICAL SIMULATION

We perform the massive Monte-Carlo simulation on the square lattice of size  $L$  to obtain the high-precision data for  $\pi_{hs}$ . We use the dual lattice shown in Fig. 2. On such lattice the critical point of the bond percolation ( $q = 1$ ) is exactly equal  $1/2$  and is not dependent on the lattice size [24]. To produce the pseudorandom numbers we use the R9689 random number generator with four taps [25]. We close each bond with a probability  $p$  and leave it open with a probability  $1 - p$ . Then we split the lattice into clusters of connected sites by using the Hoshen-Kopelman algorithm [26]. After that we check the percolation through this configuration. We average the crossing probability over  $10^7$  random bond configurations. To investigate the Potts model  $q = 2, 3, 4$  we use the Wolff [27] cluster algorithm to generate a sequence of thermally equilibrated spin configurations. For each particular inverse temperature  $\beta = \frac{1}{T}$  we flip 20000 Wolff clusters to equilibrate the system. For the spin model on the finite lattice the deviation of the pseudocritical point from the position of the critical point on the infinite lattice is smaller for Periodic Boundary Condition (PBC) rather than the Open Boundary Condition (OBC) [28, 29]. For this reason we use the PBC for the Wolff algorithm. The Monte-Carlo algorithm generates spin configurations on a torus. For a generated spin configuration we create a configuration of bonds. Each bond between sites with equal spin variable  $\sigma$  is closed with the probability  $p = 1 - \exp(-\beta)$  and is open with

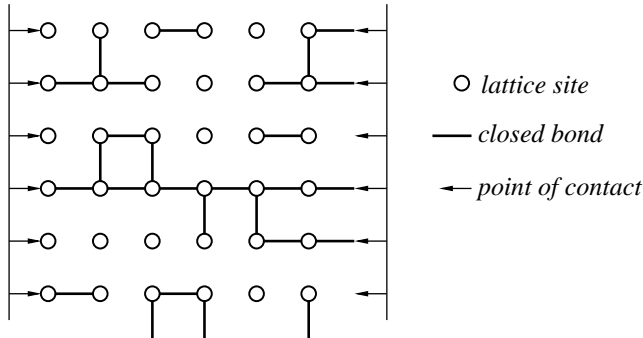


FIG. 2: The dual lattice with the horizontally spanning cluster.

probability  $1 - p = \exp(-\beta)$ . Bonds between sites with different values of  $\sigma$  are always open in accordance with Fortuin-Kasteleyn rule [1]. Then we split the particular spin and bond configurations into different clusters. Here we use OBC. It means that for each generated configuration we cut the torus and check the crossing on the square with open boundary conditions. We fix the OBC for crossing only in horizontal direction  $\pi_{hs}$  because it implies the vertical crossing is absent and the top and bottom rows must be disjointed. But we take into consideration the additional row and column of bonds, as shown in Fig. 2. We check the percolation through an obtained cluster configuration, generate new spin configuration and so on. We average the crossing probability over  $10^7$  configurations for each value of the inverse temperature  $\beta$ . So the resolution of our computations is about  $10^{-7}$ . By this way we perform numerical simulation and get a set of data for  $\pi_{hs}(p; L, q)$  for the lattice sizes  $L = 32, 48, 64, 80, 128$  and  $q = 2, 3, 4$ . The formal definition of  $\pi_{hs}(p; L, q)$  as a sum over different cluster configurations is described in [30].

For the Potts model we use the dual lattice as we do for the percolation. It means, that we take into account additional bonds attached to the bottom row of spins. In the same way we take into account additional bonds attached to the right column of the spins. On the lattice with PBC these bonds have to connect the right and the left columns. We cut the torus (because we use OBC for crossing probability) but we keep these additional bonds and take into account the checking of the crossing. In Fig. 2 contact points are shown by arrows. The left contact points are attached to the left column of sites. The right contact points are attached to additional bonds. In Fig. 2 the bond configuration with the horizontally spanning cluster is shown. Then we check the percolation through the obtained

cluster configuration. After that we flip three Wolff clusters, check spanning for a new spin configuration and so on.

### III. DETERMINATION OF THE PSEUDOCRITICAL POINT ON THE FINITE LATTICE

We investigate the crossing probability as a function of deviation from the critical point. Therefore, we perform the preliminary approximations to obtain the critical points for the finite samples. Namely, we:

- obtain the pseudocritical point and the shape of the central part of the crossing probability,
- determine the shape of the tails of the crossing probability
- combine together the information for body and tails, and reconstruct the total shape of the crossing probability.

We need to recall that we consider the crossing probability as a function of the variable  $p = 1 - \exp(-\beta)$  (probability of a bond to be closed). It is easy to understand that we must take the pseudocritical point on the finite lattice  $p_c(L, q)$  as the reference point. The crossing probability is a symmetric function of the variable  $\Delta p = (p - p_c(L, q))$ . This fact implies that the high temperature tail  $p_c - \Delta p$  ( $\Delta p > 0$ ) and the low temperature tail  $p_c + \Delta p$  coincide  $\pi_{hs}(p_c - \Delta p) = \pi_{hs}(p_c + \Delta p)$ . For the bond percolation on the dual lattice the position of the percolation point does not depend on the lattice size  $p_c(L, q = 1) = 0.5$  [24].

For the determination of  $p_c(L, q)$  for the Ising and the Potts model we use the following procedure. We can assume [30] that in the region  $-6 < \ln(\pi_{hs}(p; L, q))$  the fitting formula is true

$$F(p; L, q) = A(q, L) \exp(-[B(L, q)(p - p_c(L, q))]^{\zeta(L, q)}). \quad (2)$$

Therefore we fit the logarithm of the crossing probability  $\ln(\pi_{hs})$  by the function  $f_1(p; L, q) = \ln(F(p; L, q))$  namely

$$f_1(p; L, q) = a(L, q) - [B(L, q)(p - p_c(L, q))]^{\zeta(L, q)}, \quad (3)$$

where  $a(L, q) = \ln(A(L, q))$ . We plot the data for  $\ln(\pi_{hs}(p; L, q))$  as a function of  $p$  in Fig. 3a),

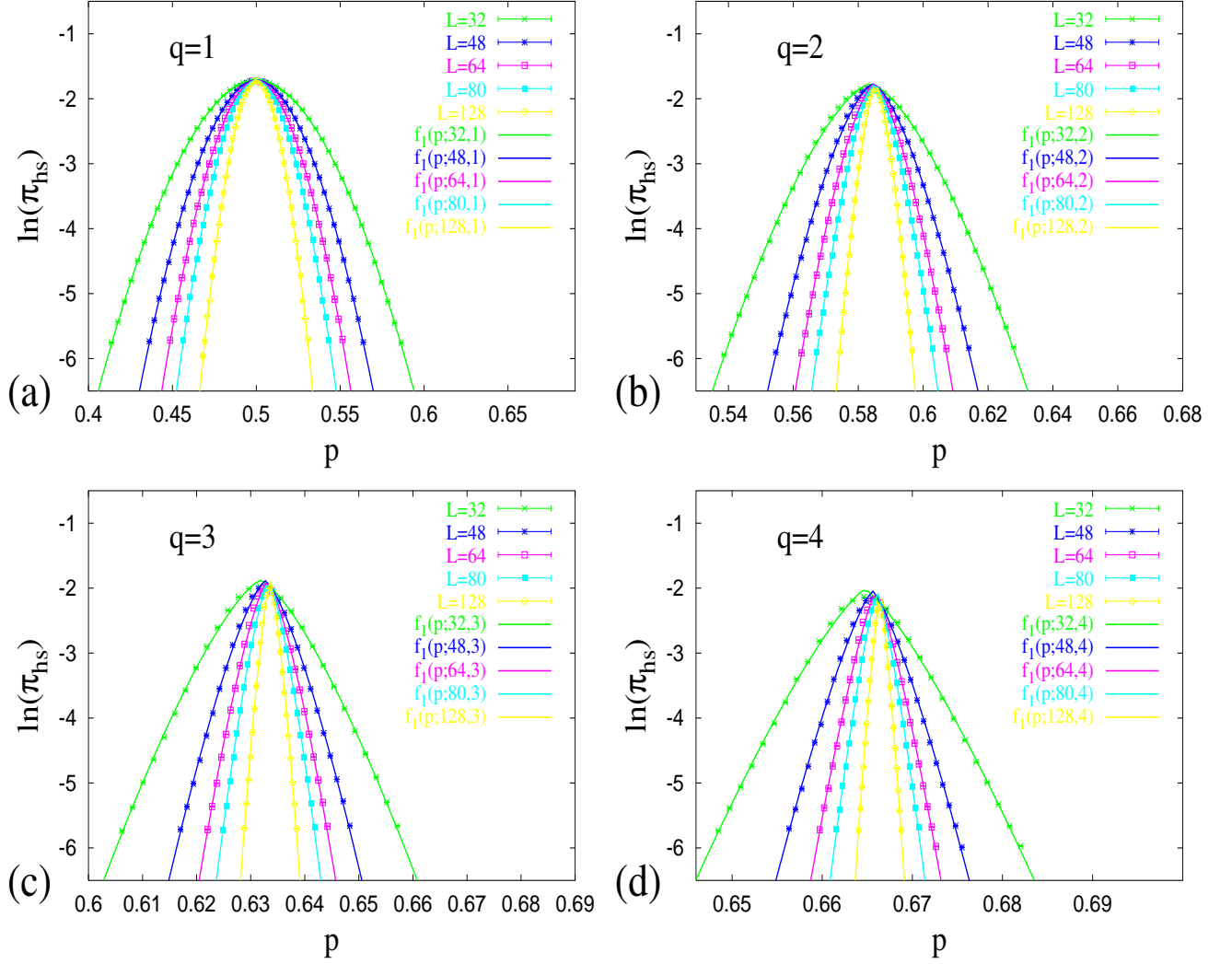


FIG. 3: Approximation of the logarithm of the crossing probabilities  $\ln(\pi_{hs})$  as a function of  $p$  by the function  $f_1(p; L, q) = a(L, q) - B(L, q)(p - p_c(L, q))^{-\zeta(L, q)}$  for: a) percolation  $q = 1$ , b) Ising model  $q = 2$ , c) Potts model  $q = 3$ , d) Potts model  $q = 4$ .

Fig. 3b), Fig. 3c), Fig. 3d) for  $q = 1, 2, 3, 4$  respectively. The errorbars in these figures are about the symbol size. It seems, that behavior of  $\ln(\pi_{hs}(p; L, q))$  near  $p_c$  is parabolic. Results of the approximation are plotted in the same figures by lines. We shall see that there is a good agreement between the numerical data and the results of the approximation. But we see deviation at the point  $p_c$  especially for  $q = 3, 4$ . In the vicinity of  $p_c$  real graphs are more smooth than fitting functions. Finally for each pair of numbers  $(L, q)$  we obtain four fitting parameters  $A(L, q)$ ,  $B(L, q)$ ,  $p_c(L, q)$ ,  $\zeta(L, q)$ . Here  $A(L, q)$  defines the crossing probability in the critical point,  $B(L, q)$  is a scaling variable,  $p_c(L, q)$  is the position of the

pseudocritical point on the lattice  $L$ , and  $\zeta(L, q)$  is a scaling index.

In Table I we collect data for the logarithm of critical amplitude  $a(L, q) = \ln(A(L, q))$ . The fitting parameter  $a(L, q)$  defines a vertical shift of graphs in Fig. 3a)-3d) from the zero level. In Table II the data for the scaling variable  $B(L, q)$  are shown. We approximate the

TABLE I: Results of the approximation for the fitting parameter  $a(L, q) = \ln(A(L, q))$ .

$L$	$q = 1$	$q = 2$	$q = 3$	$q = 4$
32	-1.708(4)	-1.773(14)	-1.881(23)	-2.022(27)
48	-1.710(4)	-1.773(16)	-1.886(27)	-2.043(30)
64	-1.711(4)	-1.776(16)	-1.894(27)	-2.055(32)
80	-1.711(5)	-1.777(17)	-1.897(27)	-2.078(29)
128	-1.705(8)	-1.777(18)	-1.898(29)	-2.089(31)

data for  $B(L, q)$  by the function  $b^*(L, q)L^{u(L, q)}$ . In Fig. 4a) the results of approximation are plotted by lines. Values of the fitting parameters  $b^*(L, q)$ ,  $u(L, q)$  as well as the inverse correlation length index  $\frac{1}{\nu}$  are placed in the three last rows of Table II. We can see for  $q = 1, 2, 3$  that  $u(L, q) \simeq \frac{1}{\nu(q)}$ . It can be assumed that

$$B(L, q) = b^*(L, q)L^{\frac{1}{\nu(q)}}. \quad (4)$$

In the case  $q = 4$  the scaling index  $u(q)$  is not equal  $\frac{1}{\nu(q=4)}$ . Many critical quantities in the Potts model  $q = 4$  exhibit logarithmic corrections [31, 32, 33, 34]. These logarithmic corrections explain the difference between analytical value  $\frac{1}{\nu(q=4)} = 1.5$  and numerical approximation for the scaling index  $u = 1.372(8)$ . The position of the critical point as a function of the lattice size  $L$  is shown in Fig. 4b). On the dual lattice the position of the critical point for percolation is equal  $\frac{1}{2}$  and does not depend on the lattice size. For our computation for all points  $p_c(L, q)$  the deviations from 0.5 are less than 0.0001. This deviation corresponds to numerical inaccuracy of our Monte-Carlo simulation. The data  $p_c(L, q)$  for  $q = 2, 3, 4$  were approximated by the power function of the lattice size  $p_c(L, q) \simeq p_c(q) + dp(q)L^{v(q)}$ . Results of approximation are placed in Table III and are also plotted by lines in Fig. 4b). We shall see that our fitting procedure determines the critical point with accuracy up to four digits after the decimal point. Thus, we shall use obtained values  $p_c(L, q)$  for following approximation of tails of the crossing probability. In Table IV we place the results of



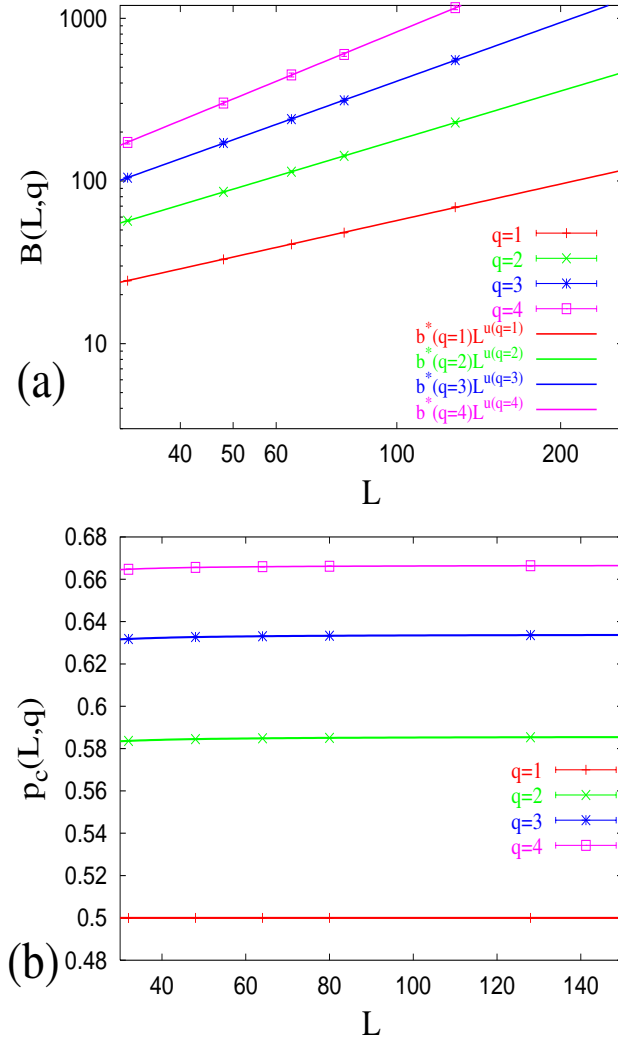


FIG. 4: a) The fitting parameter  $B(L, q)$  as a function of  $L$ . Results of the approximation by functions  $b^*(L, q)L^{u(L, q)}$  (see Table II) are plotted by lines; b) Position of the pseudocritical point on the finite lattice  $p_c(L, q)$  as a function of the lattice size  $L$  for  $q = 1, 2, 3, 4$  and approximation by the pow law  $p_c(L, q) = p_c(\infty, q) + dp(q)L^{v(q)}$  for  $q = 2, 3, 4$ . Line 0.5 is also added.

the approximation for the index  $\zeta(L, q)$  describing the curvature of the central part of the crossing probability.

TABLE II: Data for  $B(L, q)$  and fitting parameters  $b^*(L, q)$ ,  $u(L, q)$ .

$L$	$q = 1$	$q = 2$	$q = 3$	$q = 4$
32	24.8(1)	60(1)	116(3)	195(6)
32	24.4(1)	57(1)	105(2)	173(4)
48	33.0(1)	86(1)	171(4)	301(8)
64	40.8(1)	114(1)	240(5)	449(12)
80	48.2(1)	143(2)	313(7)	599(15)
128	68.9(4)	229(3)	553(13)	1163(31)
$b^*(L, q)$	1.84(2)	1.767(9)	1.63(2)	1.49(5)
$u(L, q)$	0.746(3)	1.002(1)	1.198(4)	1.372(8)
$\frac{1}{\nu(q)}$	0.75	1	1.2	1.5

TABLE III: Results of the approximation of  $p_c(L, q)$  by the power law  $p_c(q) + dp(q)L^{v(q)}$ . The analytical values  $p_c^{precise}(q) = \sqrt{q}/(\sqrt{q} + 1)$  are added for comparison.

$q$	$dp(q)$	$v(q)$	$p_c(q)$	$p_c^{precise}(q)$
2	-0.160(5)	-1.25(1)	0.58573(2)	0.585786...
3	-0.22(2)	-1.33(2)	0.63394(2)	0.633975..
4	-0.26(2)	-1.42(4)	0.66666(1)	0.6666666..

#### IV. THE SHAPE OF THE THE CROSSING PROBABILITY $\pi_{HS}$ TAILS: DIRECT APPROACH.

Let us check the shape of the crossing probability tails. The double logarithm of the crossing probability  $\ln(-\ln(\pi_{hs}(L, q)))$  are plotted as functions of the variable  $t = \ln(|p - p_c(L, q)|)$  in Fig. 5a), Fig. 5b), Fig. 5c), Fig. 5d) for  $q = 1, 2, 3, 4$  respectively. Points for high-temperature and low-temperature tails lay on the same lines. This yields that we shall prove one more time our fitting procedure.

We expect that the crossing probability tails are described by the formula

$$\pi_{hs}(p; L, q) = D(L, q) \exp\left(-C(L, q)(p - p_c(L, q))^{x(L, q)}\right). \quad (5)$$

In the interval  $\ln(6) \leq \ln(-\ln(\pi_{hs}(L, q))) \leq \ln(12)$  the tails of the crossing probability look

TABLE IV: Results of the approximation for  $\zeta(L, q)$ .

$L$	$q = 1$	$q = 2$	$q = 3$	$q = 4$
32	1.887(6)	1.52(2)	1.38(3)	1.28(3)
48	1.883(7)	1.52(2)	1.37(3)	1.27(3)
64	1.882(6)	1.52(2)	1.38(3)	1.28(3)
80	1.885(7)	1.52(2)	1.38(3)	1.30(3)
128	1.86(1)	1.52(2)	1.37(3)	1.28(3)

like straight lines.

The absence of prefactor before the exponent in Eq. (5) was argued in Ref.[17] for the case of wrapping in the horizontal direction in terms of transfer-matrix. We can not directly apply the same arguments in our case, because we consider another function – the probability of crossing only in the horizontal direction. The presence of prefactor must cause the deviation from the linear dependence in Fig. 5 in accordance with Eq. (6)

$$\begin{aligned} \ln[-\ln(\pi_{hs})] &= \ln[-d(L, q) + C(L, q) \exp(tx(L, q))] \simeq \\ &\simeq \ln(C(L, q)) + x(L, q)t - \frac{d(L, q)}{C(L, q) \exp(tx(L, q))}. \end{aligned} \quad (6)$$

Here  $d(L, q) = \ln(D(L, q))$  and  $t = \ln(|p - p_c(L, q)|)$  is a logarithm of deviation from the critical point. But deviation due to prefactor  $D(L, q) \neq 1$  exponentially decreases as  $t$  growth so it is possible to avoid the deviation from the linear dependence by appropriate choice of an interval of approximation. In the region of approximation points in Fig. 5 lie on lines with good accuracy. We obtain the set of  $p_c(L, q)$  for  $L = 32, \dots, 128$  and  $q = 2, 3, 4$  in Section III. Using this data let us approximate the double logarithm of tails  $\ln(-\ln(\pi_{hs}))$  as a function of  $t$  by formula (7)

$$f_2(t; L, q) = \tilde{c}(L, q) + x(L, q)t. \quad (7)$$

Combining (5) and (7), we obtain  $\tilde{c}(L, q) = \ln(C(L, q))$ . The resolution of our computations  $10^{-7}$  is about 16 units in  $(-\ln)$  scale and is about 2.7 units in  $(\ln(-\ln))$  scale. We use the points in the interval  $\ln(6) < \ln(-\ln(\pi_{hs})) < \ln(12)$ ,  $\ln(6) \simeq 1.79$ ,  $\ln(12) \simeq 2.48$  for this approximation. This interval is indicated in Fig. 5a)-Fig. 5d) by horizontal lines. In this figures the slope lines represent results of approximation for  $x(L, q)$ .

In the region  $\ln(-\ln(\pi_{hs})) < \ln(6)$  the crossing probability obeys another scaling formula. In the region  $\ln(-\ln(\pi_{hs})) > \ln(12)$  the numerical inaccuracy becomes large. There are

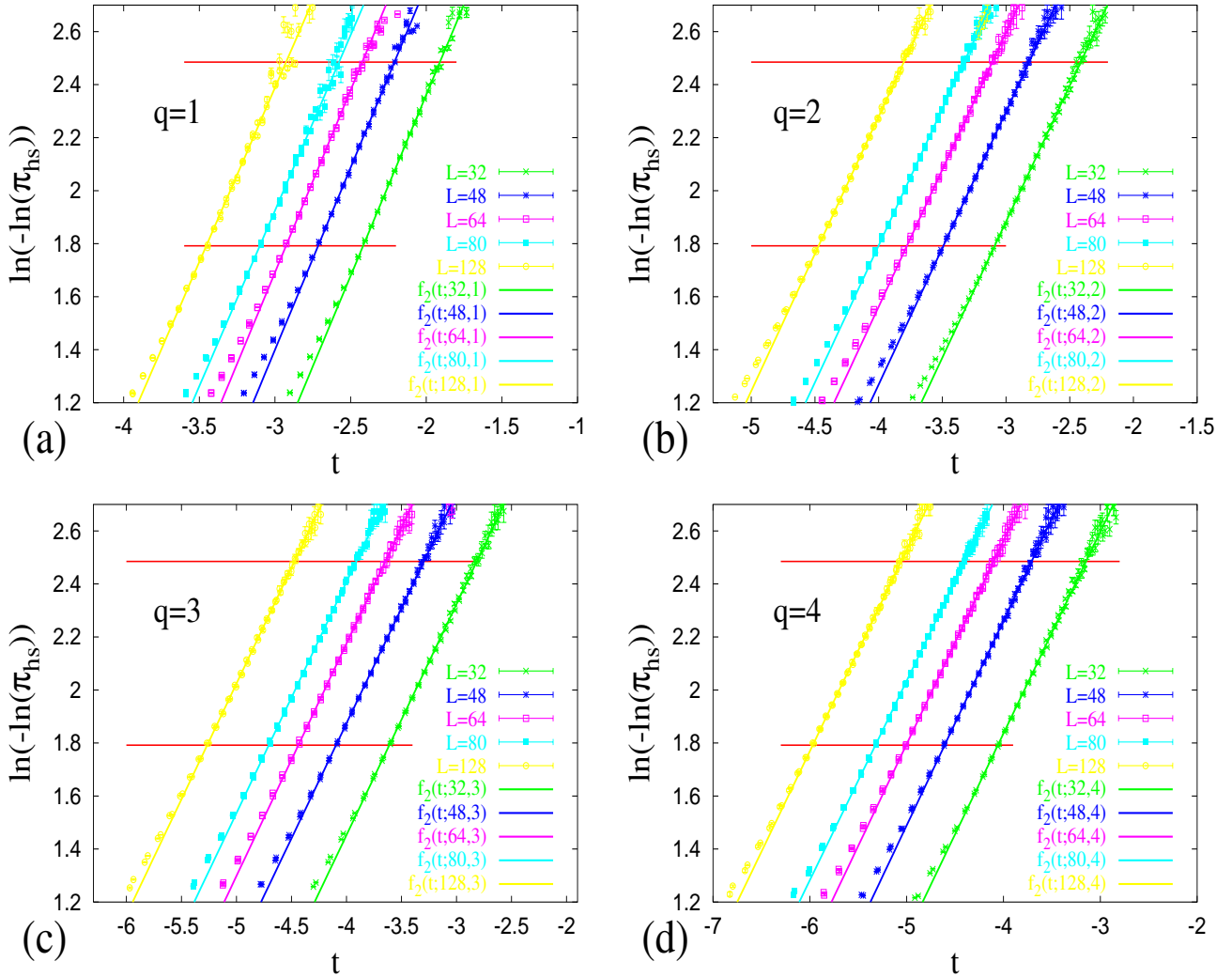


FIG. 5: Approximation of the double logarithm of the crossing probabilities  $\ln(-\ln(\pi_{hs}(p; L, q)))$  by the function  $f_2(t; L, q) = \tilde{c}(L, q) + x(L, q)t$  of the logarithm of the distance to the critical point  $t = \ln(|p - p_c(L, q)|)$  for: a) percolation  $q = 1$ , b) Ising model  $q = 2$ , c) Potts model  $q = 3$ , d) Potts model  $q = 4$ . The range of the approximation is shown by horizontal lines.

only a few numbers of “hits” in horizontally spanning clusters for  $\ln(-\ln(\pi_{hs})) > \ln(12)$ . Results of the numerical approximation for  $x(L, q)$  and  $\tilde{c}(L, q)$  are presented in Table V and Table VI respectively. As we can see  $x(L, q) \simeq \nu(q)$ . Exception is the case  $q = 4$ . For  $q = 4$  we obtain  $x(L, q = 4) \simeq 3/4$  instead of  $\nu(q = 4) = 2/3$ . This deviations can be explained by the logarithmic corrections. Some deviations exceeding the approximation errors can be explained by the choice of the approximation region. As it can be seen from Fig. 5a)–Fig. 5d) decreasing of the bottom approximation bound  $\ln(6)$  causes decreasing of

TABLE V: The slope of lines: results of the approximation for  $x(L, q)$ , the analytical values  $\nu(q)$  are presented for comparison.

$L$	$q = 1$	$q = 2$	$q = 3$	$q = 4$
$\nu$	$4/3 \simeq 1.3333$	1	$5/6 \simeq 0.83333$	$2/3 \simeq 0.6666$
32	1.366(11)	1.026(23)	0.87(2)	0.761(21)
48	1.375(10)	1.030(12)	0.868(12)	0.772(14)
64	1.376(12)	1.035(8)	0.877(8)	0.767(10)
80	1.32(3)	1.032(10)	0.872(13)	0.752(14)
128	1.31(4)	1.036(5)	0.874(6)	0.759(4)

the slope of the approximation line. From all said above we can conclude that the tails of the crossing probability behaves like  $\exp(-(p - p_c)^\nu)$ . We fit the parameter  $\tilde{c}(L, q)$  by the

TABLE VI: Shift of the lines: results of the approximation  $\ln(C(L, q)) = \tilde{c}(L, q) = c_1^* + c_2^* \ln(L)$ .

$L$	$q = 1$	$q = 2$	$q = 3$	$q = 4$
32	5.09(2)	4.96(6)	4.940(8)	4.88(8)
48	5.52(2)	5.39(4)	5.35(5)	5.35(6)
64	5.82(3)	5.70(3)	5.68(3)	5.63(4)
80	5.9(8)	5.92(4)	5.90(5)	5.79(7)
128	6.33(12)	6.42(2)	6.39(3)	6.32(2)

expression  $c_1^* + c_2^* \ln(L)$  and show results in Table VII. In Fig. 6 the fitting parameter  $\tilde{c}(L, q)$  is plotted as a function of  $L$  for  $q = 1, 2, 3, 4$ . Results of approximation  $c_1^* + c_2^* \ln(L)$  for  $q = 1, 2, 3, 4$  are added as well. We may assume that the parameter  $c_2^*$  for  $q = 1, 2, 3, 4$  is equal 1 within accuracy of the approximation. In accordance with scaling theory for the system of size  $L$  the deviation from the critical point is described by expression  $L(p - p_c)^\nu$ . Therefore we may assume that

$$\pi_{hs}(p; L, q) \simeq D(L, q) \exp\left(-c(q)L [p - p_c(L, q)]^{\nu(q)}\right). \quad (8)$$

In Fig. 1a) we show the crossover from the parabolic like functional dependence in the vicinity of the critical point to the tails. Namely, we plot the data  $-\ln(\pi_{hs})$  for  $q = 2$ ,  $L = 128$  as a function of the variable  $\tau = L(p - p_c(L, q))^\nu$ . We shall call the function

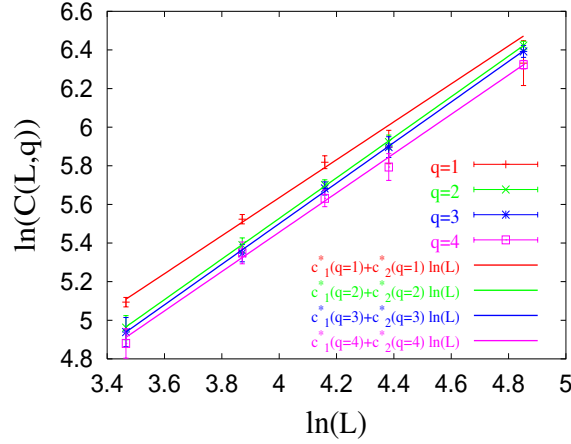


FIG. 6: The fitting parameter  $\tilde{c}(L, q) = \ln(C(L, q))$  (the vertical shift of the approximation lines for tails) as a function of  $\ln(L)$  for  $q = 1, 2, 3, 4$ . Results of approximation  $c_1^*(q) + c_2^*(q) \ln(L)$  are shown by lines.

TABLE VII: Results of the approximation of  $\tilde{c}(L, q)$  by the function  $c_1^*(q) + c_2^*(q) \ln(L)$ .

$q$	1	2	3	4
$c_1^*$	1.7(2)	1.32(12)	1.30(6)	1.38(1)
$c_2^*$	0.98(6)	1.05(2)	1.05(2)	1.02(2)

under consideration in the vicinity of the critical point a "body" of the crossing probability. Procedure of approximation for this figure is described below.

## V. NEW FITTING PROCEDURE

From the above said we can make the following conclusions. There are two scaling regions: the first one is in the vicinity of the critical point, and the second is the tails. Analyzing the Eqs. (2), (4) and (8) we can conclude that the distance from the critical point  $(p - p_c(L, q))$  and the lattice size  $L$  occur in a formula only as combination  $L/\xi \sim L(p - p_c(L, q))^{\nu(q)}$  in accordance with scaling theory. Let us introduce a scaling variable

$$\tau = L(p - p_c(L, q))^{\nu(q)}. \quad (9)$$

If we plot the negative logarithm of the crossing probability  $-\ln(\pi_{hs})$  as a function of the scaling variable  $\tau$  then we expect the power dependence in the vicinity of zero and

linear dependence for tails, as we can see in Fig. 1a). We can use the scaling variable  $\tau = L(p - p_c(L, q))^{\nu(q)}$  to fit the crossing probability taking into account the finite size scaling. Let us describe a new fitting procedure.

We may assume that we obtain the position of the critical point on the finite lattice  $p_c(L, q)$  as a result of the previous fit. Thus, we can use only three free fitting parameters and fix the value  $p_c(L, q)$ . Substituting Eq. (9) for  $\tau$  in Eq. (3) and Eq. (5), we obtain the fitting formulas for the body and the tails of the crossing probability

$$-\ln(\pi_{hs}) \simeq f_3(\tau; L, q) = -a(L, q) + b(L, q)\tau^{z(L, q)}, \quad (10)$$

$$-\ln(\pi_{hs}) \simeq f_4(\tau; L, q) = -d(L, q) + c(L, q)\tau. \quad (11)$$

Here  $\tau = L(p - p_c(L, q))^{\nu(q)}$ . If our assumptions are correct then fitting parameters  $a, d, c, z$  do not depend on the lattice size  $L$ .

The numerical value of the variable  $p_c(L, q)$  is used for computation of  $\tau$  in accordance with Eq. (9). Comparing new fitting procedures Eqs. (10), (11) and previous fitting procedures Eqs. (3), (5) we can obtain relations between new fitting parameters  $b(L, q)$ ,  $z(L, q)$ ,  $c(L, q)$  and parameters  $b^*(L, q)$ ,  $\zeta(L, q)$ ,  $C(L, q)$

$$b(L, q) = b^*(L, q)^{\zeta(q)}, \quad (12)$$

$$\zeta(L, q) = z(L, q)\nu(L, q), \quad (13)$$

$$C(L, q) = c(L, q)L, \quad \tilde{c}(L, q) = \ln(C(L, q)). \quad (14)$$

The special case is  $q = 4$ . As we can observe from the results of the approximations in Table II and Table V the finite size scaling of the crossing probability for  $q = 4$  does not obey the scaling law  $L(p - p_c)^{\nu(q=4)}$  (probably to logarithmic corrections to scaling). Therefore, instead of the analytical value  $\nu(q = 4) = 2/3$  we use the numerical approximation  $x(q = 4) = 3/4$  from Table V. We can see later, that this substitution allows us to obtain correct results for scaling.

We perform the fitting procedure in accordance with the formula proposed above. For the fit of the body of the crossing probability Eq. (10) the scaling region  $1.6 < -\ln(\pi_{hs}) < 6$  was used. For the fit of the tails of the crossing probability Eq. (11) we use the scaling region  $6 < -\ln(\pi_{hs}) < 12$ . We place results of the fitting procedure for  $q = 1, 2, 3, 4$  in Fig. 7a), Fig. 7b), Fig. 7c), Fig. 7d) respectively. In these figures the fitting regions are denoted by

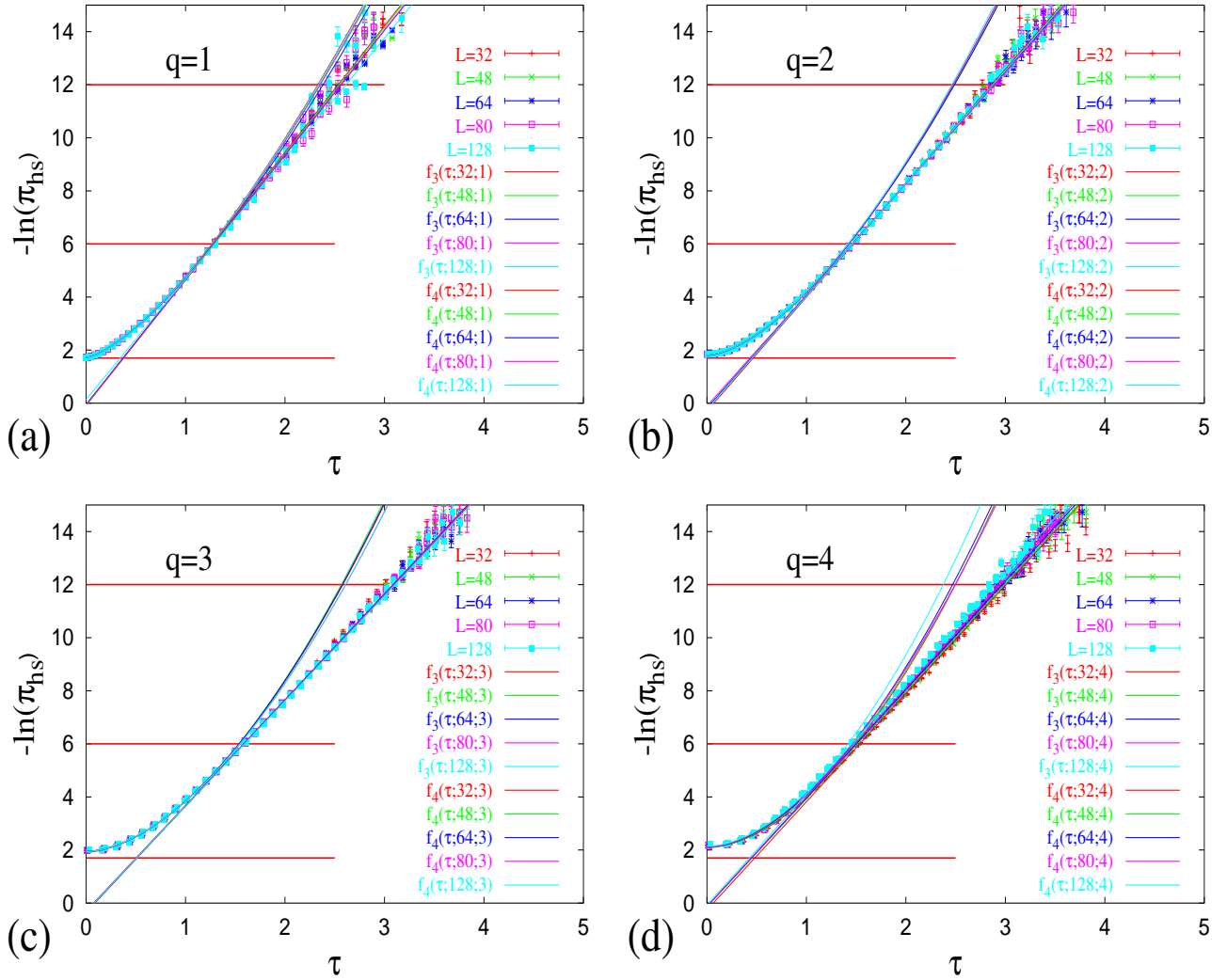


FIG. 7: The negative logarithm of the crossing probability  $-\ln(\pi_{hs}(p; L, q))$  as a function of the scaling variable  $\tau = L(p - p_c(L, q))^{\nu(q)}$  for: a) percolation  $q = 1$ , b) Ising model  $q = 2$ , c) Potts model  $q = 3$ , d) Potts model  $q = 4$ . Results of the approximation of the body of the crossing probability by the function  $f_3(\tau; L, q) = -a(L, q) + b(L, q)\tau^z$  and tails of the crossing probability by the function  $f_4(\tau; L, q) = -d(L, q) + c(L, q)\tau$  are added. The ranges of approximation regions are shown by horizontal lines.

horizontal lines. As we expect, if we plot the data as functions of the scaling variable  $\tau$  then the finite size dependence eliminates and points for different values of  $L$  lie on the same curves. Results of the approximation for the fitting parameters  $b(L, q)$ ,  $z(L, q)$ ,  $c(L, q)$  and  $d(L, q)$  are collected in Table VIII, Table IX, Table X, Table XI respectively.

The data for  $b(L, q)$  in Table VIII demonstrates, that this fitting parameter does not



depend on the lattice size  $L$ . All dependence on  $L$  is enclosed in the expression for  $\tau$ . Hence we can omit the variable  $L$  in the round brackets and consider  $b(q)$  only as a function of  $q$ . This fact proved the choice of the fitting procedure. The data in Table IX presents some

TABLE VIII: Results of the approximation for the fitting parameter  $b(L, q)$ .

$L$	$q = 1$	$q = 2$	$q = 3$	$q = 4$
32	3.063(3)	2.38(2)	1.91(2)	1.87(3)
48	3.032(3)	2.40(2)	1.89(2)	1.95(2)
64	3.018(5)	2.38(2)	1.90(2)	1.97(3)
80	3.027(5)	2.39(2)	1.91(3)	2.02(3)
128	3.049(6)	2.38(2)	1.90(3)	2.05(3)

power  $z(q)$ . This power describes the behavior of the crossing probability in the vicinity of the critical point as a function of the scaling variable  $\tau$  and does not depend on the lattice size. The data for the fitting parameter  $c(L, q)$  are placed in Table X. It seems, that this

TABLE IX: Results of the approximation for the fitting parameter  $z(L, q)$ .

$L$	$q = 1$	$q = 2$	$q = 3$	$q = 4$
32	1.432(3)	1.61(2)	1.75(3)	1.82(3)
48	1.426(4)	1.59(2)	1.77(3)	1.78(3)
64	1.413(5)	1.59(2)	1.76(4)	1.78(4)
80	1.432(4)	1.60(3)	1.73(4)	1.73(3)
128	1.432(6)	1.61(3)	1.74(4)	1.81(5)

parameter does not depend on  $L$ . The results for  $d(L, q)$  is placed in Table XI. First of all, this parameter does not depend on the lattice size within accuracy of the approximation. The absolute value of parameter  $d(q)$  is relatively small so the prefactor  $D(q)$  is about 1. For percolation the order of  $d(q = 1)$  is less than three value of numerical inaccuracy, thus it is possible  $d(q = 1) = 0$ .

TABLE X: Results of the approximation for the fitting parameter  $c(L, q)$ .

$L$	$q = 1$	$q = 2$	$q = 3$	$q = 4$
32	4.76(3)	4.29(4)	3.97(3)	4.08(4)
48	4.75(3)	4.25(1)	4.00(2)	4.06(2)
64	4.70(2)	4.23(2)	4.00(3)	4.09(2)
80	4.71(6)	4.19(3)	3.99(3)	4.12(2)
128	4.54(8)	4.26(4)	3.96(3)	4.17(2)

TABLE XI: Results of the approximation for the fitting parameter  $d(L, q)$ .

$L$	$q = 1$	$q = 2$	$q = 3$	$q = 4$
32	-0.07(4)	-0.30(7)	-0.29(5)	-0.26(7)
48	-0.10(4)	-0.21(3)	-0.35(3)	-0.14(4)
64	-0.05(3)	-0.19(4)	-0.34(6)	-0.13(3)
80	-0.06(9)	-0.11(5)	-0.33(6)	-0.13(3)
128	0.14(12)	-0.23(7)	-0.31(6)	-0.08(3)

## VI. DISCUSSION

Using the dual lattice (see Fig. 2) allows us to avoid finite size shift of the critical point for the bond percolation and to diminish it for spin models. The accuracy of definition of the critical point on the finite lattice play the principal role for the investigation of the tails scaling. The high quality of our approximation is proved by remarkable symmetry of the crossing probability with respect to the critical point  $p_c$ . In Fig. 5 and Fig. 7 we can observe that the two branches  $p - p_c > 0$  and  $p - p_c < 0$  practically coincide.

The two different scaling region of the crossing probability clearly seen in Fig. 1a) can explain the long time uncertainty about its shape. In Ref.[19] the scaling index for the percolation threshold for  $2d$  percolation model was found  $\zeta \simeq 1.9(1)$ . This result coincides with our approximation of the body of the crossing probability for percolation  $\zeta \simeq 1.864(12)$ . In more recent works [10, 16, 17, 20, 21] the tails region for percolation was investigated which is described by the scaling formula  $D \exp(-cL(p - p_c)^{\nu=4/3})$ . The crossover from to Gaussian-like behavior to slope  $4/3$  is observed in figures of Ref.[22]. It seems, near the

critical point the behavior of the crossing probability is parabolic. The rounding happens in the interval  $\tau < 0.1$ . This interval is relatively small in comparison with regions of the body  $0.1 < |\tau| < 1.5$  and tails  $1.5 < |\tau| < 4$  as it can be seen in Fig. 7.

We have five fitting parameters  $a(q)$ ,  $b(q)$ ,  $z(q)$ ,  $c(q)$ ,  $d(q)$  in expressions (10) and (11). In Fig. 7a)-Fig. 7d) we see the crossover region between the body and the tails of the crossing probability. In this region the function  $f_3$  touched the line  $f_4$ . It means, that in some point  $\tau_0$  the values of the functions are equal, therefore

$$-a(L, q) + b(q)\tau_0^{z(q)} = -d(L, q) + c(q)\tau_0, \quad (15)$$

and first derivatives of this functions are equal too

$$z(q)b(q)\tau_0^{z(q)-1} = c(q). \quad (16)$$

Substituting  $c(q)$  from Eq. (16) in Eq. (15) we obtain expression for  $b(q)$

$$b(q) = \frac{d(q) - a(q)}{(z(q) - 1)\tau_0^{z(q)}}. \quad (17)$$

If the crossing probabilities at the critical points  $A(q)$  (and logarithms  $a(q)$ ) can be calculated analytically by conformal field methods (at least for the percolation it is possible) [2, 3, 4] then only four independent parameters  $b(q)$ ,  $\tau_0(q)$  and  $z(q)$ ,  $a(q)$  remain for the crossing probability.

The main statements for the crossing probability  $\pi_{hs}$  are:

- In accordance with scaling theory the finite size scaling of the crossing probabilities may be eliminated by introducing the scaling variable  $\tau = L(p - p_c(L, q))^{\nu(q)}$ . The crossing probability as a function of  $\tau$  does not depend on the lattice size  $L$ .
- The body of the crossing probability scales  $\pi_{hs}(\tau) \simeq A(q) \exp(-b(q)\tau^{z(q)})$ .
- The tails of the crossing probabilities scales  $\pi_{hs}(\tau) \simeq D(q) \exp(-c(q)\tau)$ . The value of parameter  $D(q)$  is about 1.
- The finite size scaling for  $q = 4$  does not describe by the analytical value of the correlation length index  $\nu(q = 4) = 2/3$ . We obtain some scaling index  $x(q = 4)$ . This index  $x(q = 4) \simeq 0.759(4)$  for the tails of the crossing probability (see Table V) or  $\frac{1}{u(q)} \simeq 0.728$  for the body of the crossing probability (see Table II).

The author would like to thank Robert M. Ziff for helpful discussion and Théa Bellou for reading manuscript and for her remarks.

- 
- [1] C.M. Fortuin and P.M. Kasteleyn, *Physica* **57**, 536 (1972).
  - [2] J.L. Cardy, *Nucl. Phys. B* **275**, 200 (1986).
  - [3] J.L. Cardy, *J. Phys. A: Math. Gen.* **25**, L201 (1992).
  - [4] G.M.T. Watts, *J. Phys. A: Math. Gen.* **29**, L363 (1996).
  - [5] S. Smirnov and W. Werner, *Math. Res. Lett.* **8**, 729 (2001), e-print: math.PR/0109120.
  - [6] S. Smirnov and C. R. Acad. Sci. Paris Sr. I Math. **333**, 239 (2001).
  - [7] J.L. Cardy, *Plenary talk given at TH-2002*, e-print: cond-mat/0209638.
  - [8] R.P. Langlands, C. Pichet, P. Pouliot, and Y. Saint-Aubin, *J. Stat. Phys.* **67**, 533 (1992).
  - [9] R.P. Langlands, Ph. Pouliot, and Y. Saint-Aubin, *Bull. AMS* **30**, 1 (1994).
  - [10] R. M. Ziff, *Phys. Rev. Lett.* **72**, 1942 (1994).
  - [11] Ch.-K. Hu, C.-Yu Lin, and J.-A.Chen , *Phys. Rev. Lett.* **75**, 193 (1995).
  - [12] Ch.-K. Hu and Chai-Yu Lin, *Phys. Rev. Lett.* **77**, 8 (1996).
  - [13] C.-Yu Lin and Ch.-K. Hu, *Phys. Rev. E* **58**, 1521 (1998).
  - [14] C.-K. Hu, J.-A. Chen, and C.-Y. Lin, *Physica A* **266**, 27 (1999).
  - [15] R.P. Langlands, M.-A. Lewis, and Y. Saint-Aubin, *J. Stat. Phys.* **98**, 131 (2000).
  - [16] M.E.J. Newman and R.M. Ziff, *Phys. Rev. Lett.* **85**, 4104 (2000).
  - [17] M.E.J. Newman and R.M. Ziff, *Phys. Rev. E* **64**, 016706 (2001).
  - [18] Levinshtein, B.I. Shklovskii, M.S. Shur, and A.L. Efros, *Sov. Phys. JETP* **42**, 197 (1976).
  - [19] F. Wester, *Int. J. Mod. Phys. C* **11**, 843 (2000).
  - [20] J. Berlyand and J. Wehr, *J. Phys. A: Math. Gen.* **28**, 7127 (1995).
  - [21] J.-P. Hovi and A. Aharony, *Phys. Rev. E* **53**, 235 (1996).
  - [22] P.M.C. de Oliveira, R.A. Nobrega, and D. Stauffer, *J. Phys. A: Math. Gen.* **37**, 3743 (2004), e-print: cond-mat/0308566.
  - [23] R. J. Baxter *"Exactly Solved Models in Statistical Mechanics."*, Academic Press, 1982.
  - [24] R.M. Ziff and M.E.J. Newman, *Phys. Rev. E* **66**, 016129 (2002).
  - [25] R.M. Ziff, *Computers in Physics* **12**, 385 (1998), e-print: cond-mat/9710104.
  - [26] J. Hoshen and R. Kopelman, *Phys. Rev. B* **14**, 3438 (1976).

- [27] U. Wolff, Phys. Rev. Lett. **62**, 361 (1988).
- [28] D.P. Landau, Phys. Rev. B **13**, 2997 (1976).
- [29] D.P. Landau, Phys. Rev. B **14**, 255 (1976).
- [30] O.A. Vasilyev, Phys. Rev. E **68**, 026125 (2003).
- [31] J.L. Cardy, M. Nauenberg, and D.J. Scalapino, Phys. Rev. B **22**, 2560 (1980).
- [32] J. Salas and A.D. Sokal, J. Stat. Phys **92**, 729 (1998).
- [33] J. Asikainen *et. al.*, Eur. Phys. J. B **34**, 479 (2003), e-print: cond-mat/0212216.
- [34] J. Cardy and R. Ziff, J. Stat. Phys. **110**, 1 (2003) , e-print: cond-mat/0205404.